BBA - Biomembranes 1862 (2020) 183361

Contents lists available at ScienceDirect

BBA - Biomembranes

journal homepage: www.elsevier.com/locate/bbamem

The effect of lipid phase on liposome stability upon exposure to the mechanical stress

Joanna Doskocz[a,*,1], Paulina Dałek[a,b,1], Aleksander Foryś[c], Barbara Trzebicka[c], Magdalena Przybyło[b], Luka Mesarec[d], Aleš Iglič[d,e], Marek Langner[b]

[a] Department of Biomedical Engineering, Faculty of Fundamental Problems of Technology, Wrocław University of Science and Technology, 50-377, Wrocław, pl. Grunwaldzki, 13, Poland
[b] Lipid Systems sp. z o.o., 54-613 Wrocław, ul. Krzemieniecka 48C, Poland.
[c] Centre of Polymer and Carbon Materials, Polish Academy of Sciences, 41-819 Zabrze, ul. M. Curie-Skłodowskiej 34, Poland.
[d] Laboratory of Physics, Faculty of Electrical Engineering, University of Ljubljana, SI-1000 Ljubljana, Tržaška 25, Slovenia.
[e] Laboratory of Mass Spectrometry and Proteomics, Institute of Biosciences and BioResources, National Research Council, 80131 Napoli, Pietro Castellino 111, Italy.

ARTICLE INFO

Keywords:
Liposomes
Membrane mechanics
Lipid phase transition
Extrusion

ABSTRACT

Mechanical properties of a lipid bilayer are parameters determined mainly for giant unilamellar vesicles (GUVs). It is not clear if values obtained on the GUV model can be directly translated to submicron large unilamellar vesicles (LUVs). This ambiguity is a major obstacle in exploring the effect of lipid bilayer mechanics on membrane associated processes and effectiveness of liposome-based targeted drug delivery systems. In presented work extrusion, which is a common method to prepare LUVs, was used to study liposomes preparation and stability upon exposure to mechanical stress. The effect of parameters of the extrusion process (temperature, membrane pore size, extrusion force and volumetric flux) on the properties of liposome suspension (average liposome size, polydispersity index and lipid recovery ratio) was determined for model liposomes composed of DPPC lipid. The state of the DPPC lipid bilayer depends on temperature, therefore, the effect of lipid bilayer mechanics on the extrusion process can be quantitated without altering membrane composition. The extrusion process was carried out with the automated extruder delivering quantitative data on the extrusion force and volumetric flux. Obtained results have been interpreted in terms of mechanical properties of the lipid bilayer. Determined mechanical properties of the lipid bilayer and its dependence on temperature are in good agreement with the literature results determined for GUVs. This shows that mechanical properties of the lipid bilayer does not depend on the liposome size in the range from 100 nm to hundreds of microns.

1. Introduction

Liposomes are self-assembled lipid vesicles with diameters ranging from 50 nm to 250 μm [1] and can be formed from a large variety of amphiphilic compounds, among which phospholipids have a special place due to their biocompatibility [2]. Size, properties of aqueous phase and molecular composition of liposomes are major factors affecting their attributes including: lateral and transmembrane molecular organization, permeability, mechanical resilience and surface properties, such as propensity for hydrogen bond formation, electrostatics or steric barrier formed by surface decorations [3–6]. Consequently, a variety of liposomes can be constructed for basic research and a variety of applications [7]. Vesicles with a diameter > 1 μm are used as a convenient model of biological membrane for the determination of mechanical or topological properties [8]. Smaller liposomes with a diameter between 100 and 1000 nm have much broader applications. They are used as experimental model systems, biosensors or as a scaffold for nano-pharmaceuticals [7]. The design of a successful experimental model or effective drug delivery system requires that the selected properties of a lipid bilayer can be tuned to the required physiological values. It has been demonstrated that liposome stability, organization of lipids in the bilayer, permeability and mechanical properties depend on their molecular composition and physical state [9–12]. Whereas lipid organization and surface electrostatics are frequently studied [13,14], the effect of lipid bilayer mechanics is rarely considered, despite experimental evidences demonstrating that shape and stiffness of particulates affect their performance on both cellular and physiological levels [15,16]. This is because a limited number of

* Corresponding author.
E-mail address: Joanna.Doskocz@pwr.edu.pl (J. Doskocz).
[1] Authors contributed equally.

https://doi.org/10.1016/j.bbamem.2020.183361
Received 6 September 2019; Received in revised form 25 March 2020; Accepted 11 May 2020
Available online 15 May 2020

technically demanding experimental methodologies, capable to quantitate membrane mechanical properties, are available [17,18]. Mechanics of biological membranes and microscale artificial bilayers are studied using image analysis of strained or freely-fluctuating membrane [8,19,20]. Whereas studies using macrovesicles and biological membranes as experimental models provide data useful for understanding biological systems, there are limited number of values for evaluation of liposomes in submicron scale. Mechanical properties of such objects can be evaluated using methods relying on the measurement of a mechanical wave propagation through aqueous vesicle suspension. However, these method provides quantitative values, which are heavily dependent on theoretical model used [21]. The other approach relies on the atomic force microscopy technique, where the local, atomic level, deformations of membrane are measured [18,22,23]. In this case, the vesicle immobilisation method and the interaction of liposome with the measuring tip are sources of serious uncertainties. In the paper, we present the new experimental technique, which can deliver data on mechanical properties of liposomes in suspension with sizes below the resolution limit of optical microscopy. To demonstrate the method viability a well-characterized experimental system, whose mechanical properties change with temperature, has been used. Liposomes formed from 1,2-dipalmitoyl-sn-glycero-3-phosphocholine (DPPC) have the main phase transition at about 41 °C [24]. Above the main phase transition temperature, the lipid bilayer is in the fluid phase where alkyl chains are disordered. The bending rigidity of the lipid bilayer is low and has been determined to be equal to about 10^{-19} J [25]. When the temperature is below the main phase transition, the alkyl chains are stabilized by van der Walls interactions making lipid bilayer mechanically resilient [24,26]. At temperatures between 33.5 °C and 41 °C lipid bilayer is at the ripple phase characterized by corrugations of the membrane surface with well-defined periodicity with an axis parallel to the mean bilayer plane [27]. Below 33.5 °C the lipid bilayer enters the gel state [24,28]. It has been shown previously that properties of the DPPC lipid bilayer such as area per lipid molecule, bilayer thickness or bending rigidity are temperature dependent [25,29]. In the presented research, the liposome propensity for deformation has been qualitatively and quantitatively evaluated by measuring the force needed to push preformed uniform liposomes through well-defined pores, which sizes are smaller than vesicles diameter. For that purpose, the dedicated automatic mechanical extruder, equipped with strain gauges and temperature control, was used. The liposome size and topology were monitored using the Dynamic Light Scattering technique and Cryogenic Transmission Electron Microscopy.

2. Materials and methods

2.1. Materials

1,2-dipalmitoyl-sn-glycero-3-phosphocholine (DPPC) was purchased from Avanti Polar Lipids (Alabaster, USA). Chloroform was obtained from VWR (USA). Ferric chloride hexahydrate and ammonium thiocyanate was purchased from Chempur (Poland). In all experiments 18 mΩ deionized water was used (PolWater, Poland).

2.2. Preparation and characterization of liposomes

The sample preparation procedure was divided into steps to clarify the design of the experiment. A schematic presentation of experimental design is visualised in Fig. 1.

2.2.1. MLVs preparation

Multilamellar DPPC vesicles (MLVs) were prepared by the dry film method [30]. First, lipid was dissolved in chloroform. The organic solvent was removed by the stream of argon and the residues of chloroform were eliminated under low-pressure storage. The resulting dry lipid film was hydrated overnight in deionized water at 60 °C [31] followed by vortexing. The final concentration of lipid in the sample equalled to 10 mg/mL.

2.2.2. LUVs preparation

MLVs suspension with lipid concertation equals to 1 mg/mL was extruded through polycarbonate membrane with 50 nm pores (NucleporeCorp., USA). The sample was passed through the filter once, at temperature in the range from 20 °C to 50 °C, for the characterization of the extrusion process.

2.2.3. LUVs recalibration

In the first step, the suspension of MLVs was extruded through a 100 nm polycarbonate membrane (NucleporeCorp., USA) at 50 °C. 7 cycles of extrusion (passages through the filter) were used to obtain uniform population of LUVs on the trans-side of the extrusion membrane. The measuring device contains two syringes (Fig. 2), the syringe where the MLV vesicles are loaded is called the cis-side, whereas the other syringe is call the trans-side. The diluted (1 mg/mL of lipid) LUVs suspension was extruded seven times through a 50 nm polycarbonate filter. The number of extrusion cycles was experimentally determined. Three extrusion cycles are sufficient to produce vesicles suspension characterized by the size distribution and polydispersity index, which are little altered by subsequent extrusion cycles. Similar conclusions were presented elsewhere [32]. The recalibration procedures were performed at temperatures ranging from 20 °C to 50 °C.

The extrusion and recalibration were carried out using home-made automated mechanical extruder (Lipid Systems Ltd., Wrocław, Poland). Sizes and polydispersity indexes of extruded LUV vesicles were determined using the Dynamic Light Scattering method (DLS) (Zetasizer Nano ZS, Malvern, UK). For that purpose, samples were diluted 50 times with deionized water. The deionized water was filtered through the cellulose membrane with 0.2 μm pores (VWR, USA).

2.3. The determination of lipid concentration

The concentration of DPPC was determined with the Stewart method [33]. The method is based on the formation of a colour complex between phospholipids and ammonium ferrothiocyanate. The lipid quantity in then determined by measuring the absorbance at 470 nm. Specifically, 40 μL solution containing lipids was mixed with 2 mL of chloroform and the 2 mL of aqueous solution containing 0.4 M ammonium ferrothiocyanate and 0.1 M ferric chloride hexahydrate. Mixtures were vortexed for 1 min followed by incubation for 15 min. The lower chloroform phase was transfer to quartz cuvettes (Hellma, Germany) and its absorbance was measured using spectrophotometer (SPECTROstar Nano, BMG LABTECH, Germany). The concentration of DPPC was determined based on the calibration curve.

2.4. Cryogenic Transmission Electron Microscopy (TEM) imaging

Cryogenic Transmission Electron Microscopy (cryo-TEM) images were obtained using a Tecnai F20 X TWIN microscope (FEI Company, Hillsboro, Oregon, USA) equipped with field emission gun, operating at an acceleration voltage of 200 kV. Images were recorded on the Eagle 4 k HS camera (FEI Company, Hillsboro, Oregon, USA) and processed with TIA software (FEI Company, Hillsboro, Oregon, USA). Specimen preparation was done by vitrification of the aqueous solutions on grids with holey carbon film (Quantifoil R 2/2; Quantifoil Micro Tools GmbH, Großlöbichau, Germany). Prior to use, the grids were activated for 15 s in oxygen plasma using a Femto plasma cleaner (Diener Electronic, Ebhausen, Germany). Cryo-samples were prepared by applying a droplet (3 μL) of the suspension to the grid, blotting with filter paper and immediate freezing in liquid ethane using a fully automated blotting device Vitrobot Mark IV (FEI Company, Hillsboro, Oregon, USA). After preparation, the vitrified specimens were kept under liquid nitrogen until they were inserted into a cryo-TEM-holder Gatan 626

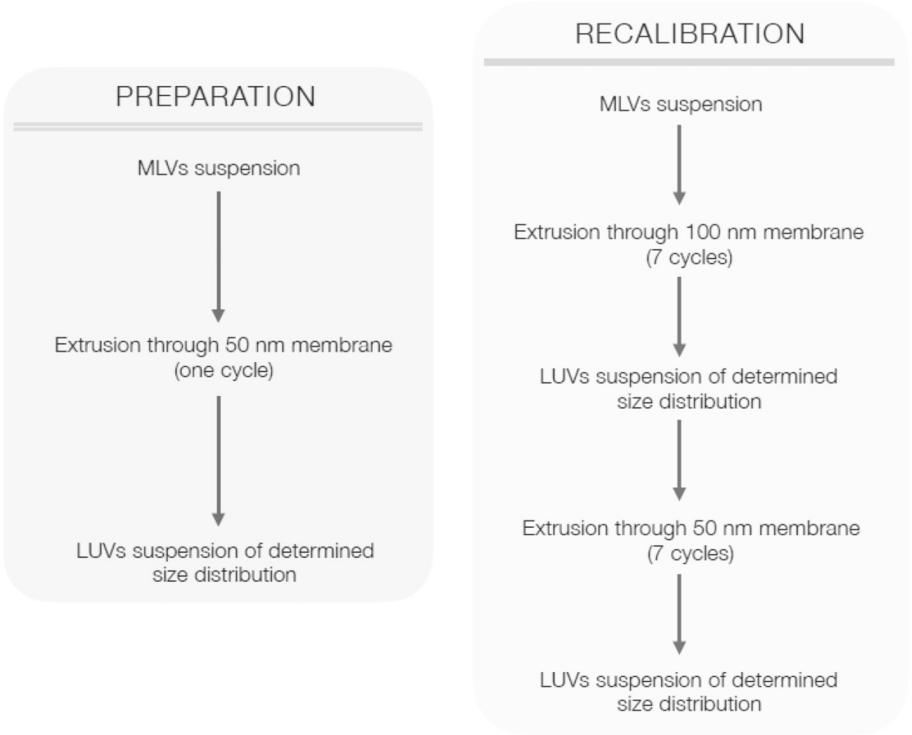

Fig. 1. The overview of two experimental protocols used in the paper. The left panel presents procedure used for the characterization of the extrusion process, where the suspension of multilamellar vesicles is transform to the suspension of unilamellar liposomes on the trans side of the filter. Right panel shows procedure employed for the characterization of membrane stability and mechanical resilience. The uniform suspension of unilamellar vesicles is produced on the trans side of the filter, following repetitive extrusion at the temperature above the lipid main phase transition. The uniform liposome suspension is than recalibrated through the filter with pores (50 nm) smaller then dimension of liposomes (140 nm).

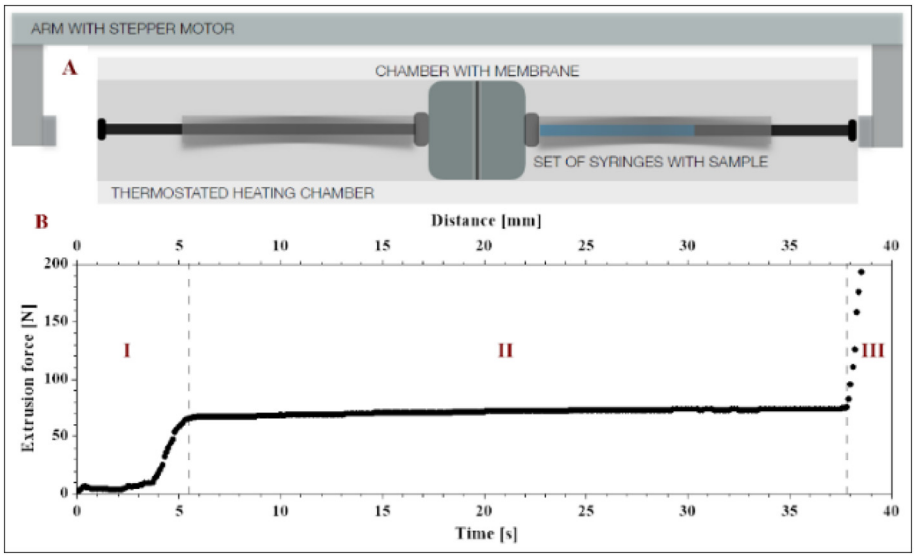

Fig. 2. The schematic diagram showing the automated extrusion device (A) and an example of the dependence of the extrusion force on time (B). The extrusion process is arbitrary divided into three stages. The "extrusion force" is define as the average value of forces in the second stage of the process. The extrusion process was carried out in isothermal conditions and at a constant volumetric flux.

(Gatan Inc., Pleasanton, USA) and analyzed in the TEM at −178 °C.

2.5. Experimental design

The force required to push liposome suspension through the polycarbonate filter was measured using dedicated home-made automated extruder (Lipid Systems Ltd., Wrocław, Poland). The design of the device is schematically illustrated in Fig. 2A. During extrusion, the temperature of the sample was tightly controlled (± 0.1 °C) and the volumetric flow rate (dV/dt) through the extrusion membrane was set in advance and maintained during the experiment with the precision motor. During the extrusion process, the force applied to a syringe was continuously measured, allowing for the construction of curves demonstrating the dependence of the force on time/distance/volumetric flux. To prevent the destruction of glass syringes an upper limit was imposed on the applied force (190 N). An example of the raw experimental data is presented in Fig. 2B. The dependence of the force on time/distance/volumetric flux can be arbitrarily divided into three stages; the rapid force increase, the steady-state stage and final force rise due to the completion of the sample transfer. The term "extrusion force", used throughout the paper, equals to the average force value of the second stage of the experimental curve. The volumetric flux (J_V) across the polycarbonate filter, the instrumental parameter, was determined from the following dependence:

$$J_V = \frac{D_s^2 \bullet v_p}{D_F^2}\left[\frac{mL}{\min \bullet cm^2}\right] \quad (1)$$

where D_F and D_S indicate the filter and syringe diameters, respectively. The velocity of the piston in the syringe is labelled as v_p and is set in advance before each experiment.

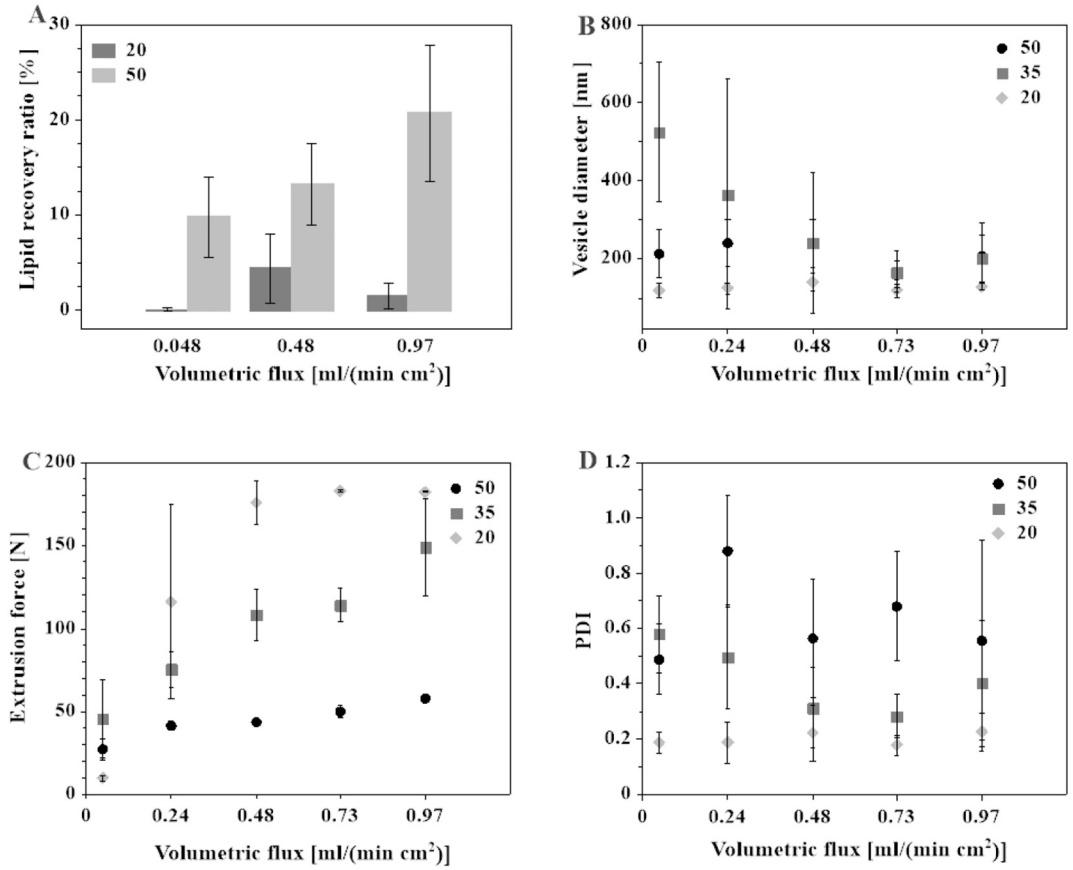

Fig. 3. The effect of temperature and volumetric flux on properties determined for a suspension of DPPC vesicles after a single extrusion cycle. MLVs were extruded once through 50 nm membrane at temperatures indicated. Panel A shows the dependence of the quantity of lipid transferred across the polycarbonate filter after a single passage as a function of volumetric flux for two temperatures (20 °C and 50 °C, labelled as dark and light gray, respectively). Panel B shows the average size of lipid vesicle as a function of volumetric flux and temperature. Panel C presents the "extrusion force" as a function of volumetric flux, and panel D the dependence of the polydispersity index of liposome suspension on the volumetric flux for three temperatures (20 °C, 35 °C and 50 °C, labelled as rhombuses, squares and circles, respectively).

3. Results and discussion

3.1. The effect of extrusion parameters on the liposome formation process

The formation of unilamellar liposomes from multilamellar structures using extrusion method is still not well understood. The process likely depends on lipid membrane elasticity, cohesion and ability to accommodate the water flow. The efficient extrusion of liposomes requires lipids to be in the fluid phase. In addition, in order to form a uniform liposome suspension, the process needs to be repeated several times [34]. Using the quantitative extrusion device, the effect of temperature and volumetric flux on the single extrusion process was investigated (Fig. 1A). Temperatures were selected so DPPC vesicles were in liquid, ripple or gel phases (50 °C, 35 °C and 20 °C). The liposome formation process was quantitated with the extrusion force, lipid recovery ratio, the average liposome size and the homogeneity of liposome population (the polydispersity index). Fig. 3A shows that following the first passage the quantity of lipids in the trans syringe does not exceed 20% of the initial lipid quantity. As expected, the lipid recovery ratio (the ratio of lipid quantity on the trans side of the filter to the total lipid quantity in the sample), when liposomes are in the fluid state, is an order of magnitude higher than that in the gel phase. There is no significant difference in the average size of liposomes as a function of a volumetric flux when lipid is in the gel or fluid phase (Fig. 3B).

Only when lipid is in the ripple phase (35 °C), the size of vesicles increases from 200 nm up to about 500 nm for small volumetric fluxes. The force required to maintain the constant volumetric flux depends both on the extrusion temperature and the preset value of the volumetric flux. As shown in Fig. 3C, when lipid is in the fluid phase, the extrusion force is the smallest and change little with the volumetric flux. When lipid is in the gel phase, the force reaches the limiting value when the volumetric flux equals 0.48 [m*L*·min^{-1}·cm^{-2}]. When the extrusion process is carried out at temperature where the lipid bilayer is in the ripple phase (35 °C) the extrusion force increases monotonically with rising volumetric flux. Presented data show, in agreement with previous observations [35], that to ensure the efficient liposome formation the suspension of MLVs should be at temperature, where lipid is in the fluid phase (41 °C or above for DPPC). Bellow the temperature of the main phase transition the lipid recovery ratio decreases dramatically and the extrusion force increases above the preset limiting value (Fig. 3A). In addition, the extrusion process of lipid in the gel or the ripple phases depends on the volumetric flux, whereas when lipid is in the fluid phase the extrusion parameters (except the lipid recovery ratio) do not depend on the volumetric flux much. In summary, the evaluation of the liposome formation process using extruder capable to provide quantitative parameters of the process agrees with previous observations that the liposome formation, when lipid is in the gel phase, is very inefficient. Less than few percent of lipid are found in the trans side of the membrane, when lipid is in the gel phase. The unexpected outcome of these experiments is that, when lipid is in the fluid phase, the lipid quantity in the trans side of the membrane, after a single pass, increases with rising volumetric flux without sacrificing the quality of liposome suspension, as evaluated with the average vesicle size and the polydispersity index.

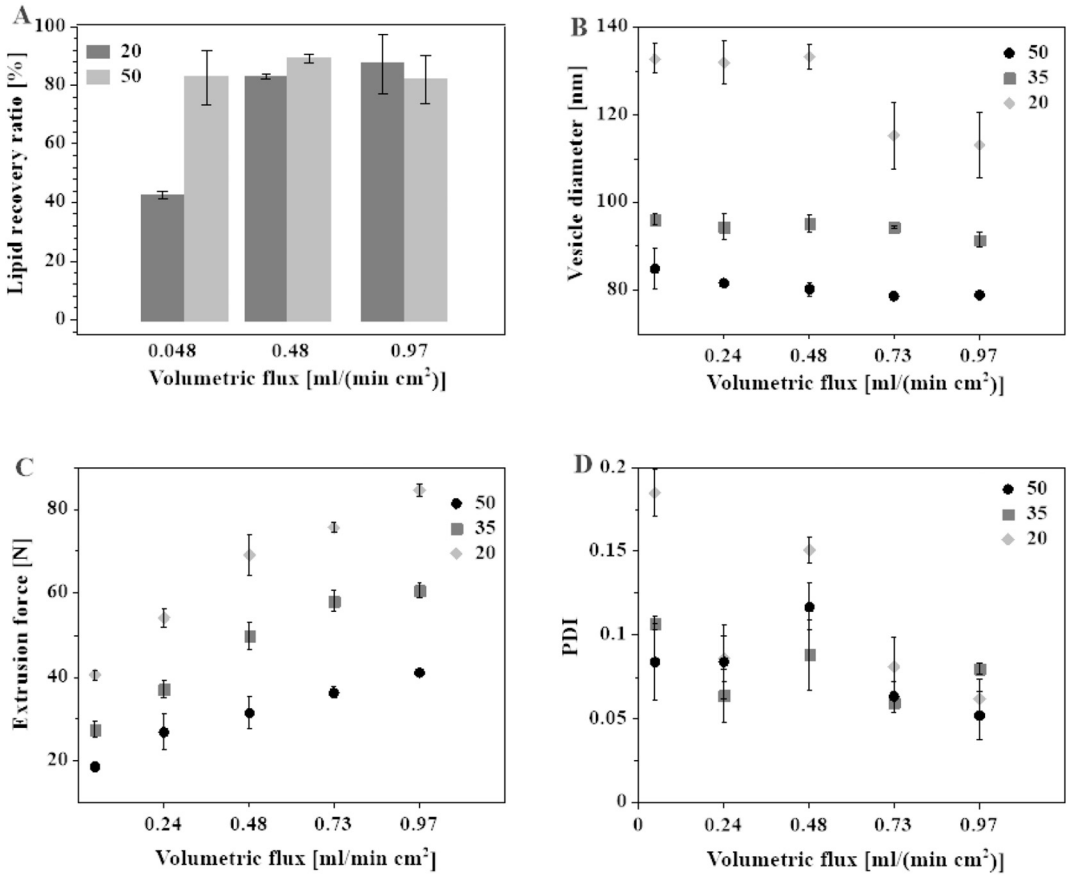

Fig. 4. Recalibration of DPPC vesicles. Preformed LUVs with average diameter equal to 138 nm were pushed 7 times through the filter with 50 nm pore size. Panel A shows the dependence of the quantity of lipid transferred across the polycarbonate filter in a single passage as a function of volumetric flux for two temperatures (20 °C and 50 °C), labelled as dark and light gray, respectively. Panel B shows the dependence of the average size of vesicles on the volumetric flux, panel C shows the dependence of the extrusion force on the volumetric flux at three temperatures and panel D the polydispersity index of liposomes in suspension extruded at different volumetric fluxes and temperatures (20 °C, 35 °C and 50 °C, labelled as rhombuses, squares and circles, respectively).

3.2. The deformability and stability of DPPC liposomes

When a homogenous population of liposomes is exposed to mechanical stress during the recalibration process (LUVs are forced through pores of significantly smaller sizes [36]) their stability and deformability can be evaluated. First, the effect of recalibration conditions (temperature and volumetric flux) on parameters of liposome suspension, such as extrusion force, lipid recovery ratio, liposome average size and polydispersity index, was measured.

Fig. 4A shows that the lipid recovery ratio during recalibration is little affected by temperature. Only when liposomes are in the gel phase and the volumetric flux is lowest (0.048 mL/min·cm^2) the lipid recovery decreases. Interestingly, the average size of liposomes after recalibration (Fig. 4B) depends on temperature. When lipid is in the fluid (50 °C) or ripple (35 °C) phases the size of liposomes is reduced from about 140 nm down to about 80 nm and 95 nm, respectively. At the two temperatures, there is a little effect of the volumetric flux on the liposomes size. When lipid is in the gel phase the outcome is different. After recalibration, the average size of liposomes decreases slightly from 140 nm down to about 110 nm, but only for high volumetric fluxes. When volumetric flux is smaller than 0.48 [mL·min^{-1}·cm^{-2}] the recalibration of liposomes in the gel phase does not change their sizes at all.

The slight decrease of vesicle diameters with increasing volumetric flux at temperatures 35 °C and 50 °C (Fig. 4B) might be affected by so-called lift force which pushes the vesicles away from the inner wall of the pore [37] and induces the formation of lubrication layer between the inner wall of the pore and the vesicle. The thickness of lubrication layer increases with increasing velocity of the vesicles [38], therefore it is expected that the diameter of the moving vesicles in the extrusion pore decreases with increasing velocity of the vesicles [39], i.e. with increasing volumetric flux. When the extrusion force is measured (Fig. 4C) its value decreases with decreasing volumetric flux at all three temperatures. At the same value of the extrusion force, the volumetric flux is larger at higher temperatures (Fig. 4C).

Experimental results presented in Fig. 4C can be qualitatively well-understood in terms of the Poiseuille-Hagen law. Since the diameter of the syringe (D_S) is much larger than the diameter of the pore (D_P), the fluidic resistance of the pore is much larger than the fluidic resistance of the syringe. Therefore, the fluidic resistance of the syringe can be neglected. When the flow of vesicle suspension through the extrusion pore/filter of the length L and constant radius $R_P = D_P/2$ is laminar the volumetric flux ($\phi_V = dV/dt$) through the extrusion pore can be described with Poiseuille-Hagen law

$$J_V = \frac{\phi_V}{\pi R_P^2} = \langle v \rangle = \frac{\Delta p\, R_P^2}{8\eta L} \tag{2}$$

where $\phi_V = dV/dt$ is the rate of the volumetric flux, η is the effective viscosity, $\langle v \rangle$ is the average velocity of the suspension of vesicles which equals to the half of the maximal velocity at the middle of the cylindrical pore (v_0), i.e. $\langle v \rangle = v_0/2$. Assuming that extrusion force equals $F_{ext} = \Delta p\, \pi {R_P}^2$, it follows from Eq. (2) that.

$$F_{ext} = [8\pi\eta L\,]\, J_V \tag{3}$$

The linear relation between extrusion force F_{ext} and the volumetric flux J_V, as given by Eq. (3) can be observed in the Fig. 4C.

Table 1
Calculated value of the effective viscosity ($L = 15$ μm).

	Temperature [°C]	Effective viscosity $\eta \cdot 10^8 \left[\frac{kg}{m \cdot s}\right]$
Preparation	20	27.6
	35	16.7
	50	4.78
Recalibration	20	7.51
	35	6.00
	50	3.72

Slopes of experimental dependencies of F_{ext} on J_V in Fig. 4C are proportional to the effective viscosity of the vesicle suspension. Assuming the validity of the Eq. (3) we can therefore conclude from Fig. 4C that the effective viscosity of the vesicle suspension decreases with rising temperature (Table 1), which is an expected result. The slight deviations from linearity in experimental dependencies of F_{ext} on flux J_V (Fig. 4C) appear only at lower temperatures (20 °C and 35 °C) and higher values of the volumetric flux J_V, where the influence of vesicle on the effective viscosity of vesicle suspension is expected to become more important. Presented experimental results indicate that the mechanical stress imposed on vesicles during recalibration affects considerably the average liposome size.

To explore the dependence of the LUVs preparation and recalibration processes on temperature in greater details the volumetric flux was fixed at 0.48 [mL·min^{-1}·cm^{-2}] and the vesicles average sizes and extrusion force were measured as a function of temperature. Fig. 5A shows that the average diameter of extruded vesicles changes with temperature. When lipid is in the gel phase (below 34 °C) liposome sizes match the size of pores in the membrane. The liposome population is very uniform and variations between different preparations are also small. It has to be remembered, however, that the lipid recovery ratio in this case is very low, as shown in Fig. 3A. When the temperature of the extrusion process increases above the pretransition temperature the sizes of extruded vesicles increase by a factor of two together with rise in variations between samples. The PDI of vesicle population extruded at gel phase is smaller than 0.25, whereas when liposomes are extruded at the ripple phase their PDI increases dramatically (> 0.5). When the extrusion force is measured (Fig. 5C) its dependence on temperature follows the general intuition. The lower the temperature the larger the extrusion force is required. When the liposome formation process was carried out at temperatures above the main phase transition the lipid recovery rate is much higher but the quality of the liposome population is very poor. In order to obtain uniform liposome population (average size and PDI equal 138 nm and 0.18, respectively) the extrusion process needs to be repeated several times. At the same time, the recovery ratio increases above 90%. These results are in good agreement with observations presented by others, showing for example that mechanically resilient liposomes (such as these containing cholesterol) are not able to pass the filter unaltered (with the anticipated level of cholesterol) [32,40]. The dependence of liposome properties (lipid recovery ratio, liposome size and PDI) on extrusion conditions (the volumetric flux, extrusion force and temperature), when determined for lipid, which properties strongly depend on temperature (DPPC), shows that the state of the lipid has a significant effect on the extrusion process indicating that it depends on the balance of two mechanical properties of the lipid bilayer: a propensity for deformation and cohesiveness. When lipid is in the fluid phase the bilayer can be deformed easily but its cohesiveness, which depends mainly on short-range van der Waals forces between hydrocarbon chains, is very weak allowing liposome recalibration. When lipid is in the gel phase the situation is different, the lipid bilayer mechanical resilience for deformation increases sharply at the main

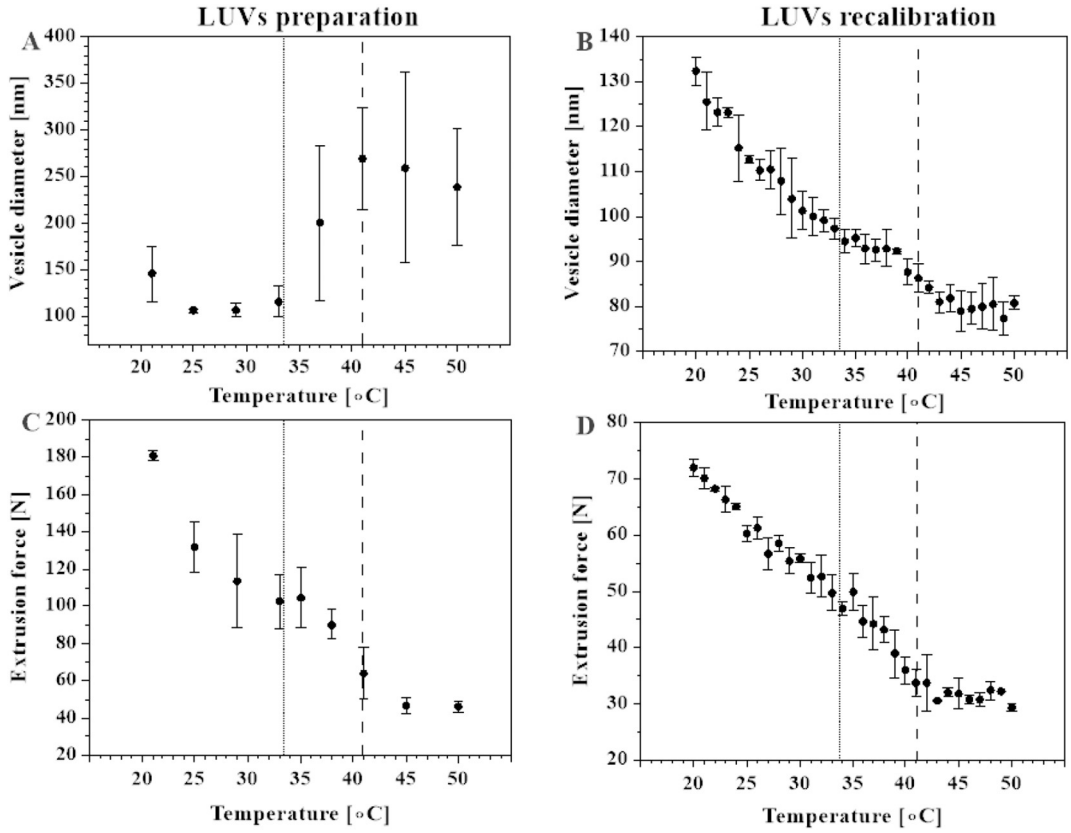

Fig. 5. The effect of the extrusion temperature on the DPPC liposome average size and the extrusion force after LUVs preparation (A, C) and LUVs recalibration (B, D) processes. The extrusion was carried out once at the volumetric flux equals to 0.48 [mL·min^{-1}·cm^{-2}]. Solid and dotted lines indicate the pretransition and the main phase transition temperatures, respectively. Error bars were calculated as a standard deviation from the average of the three samples.

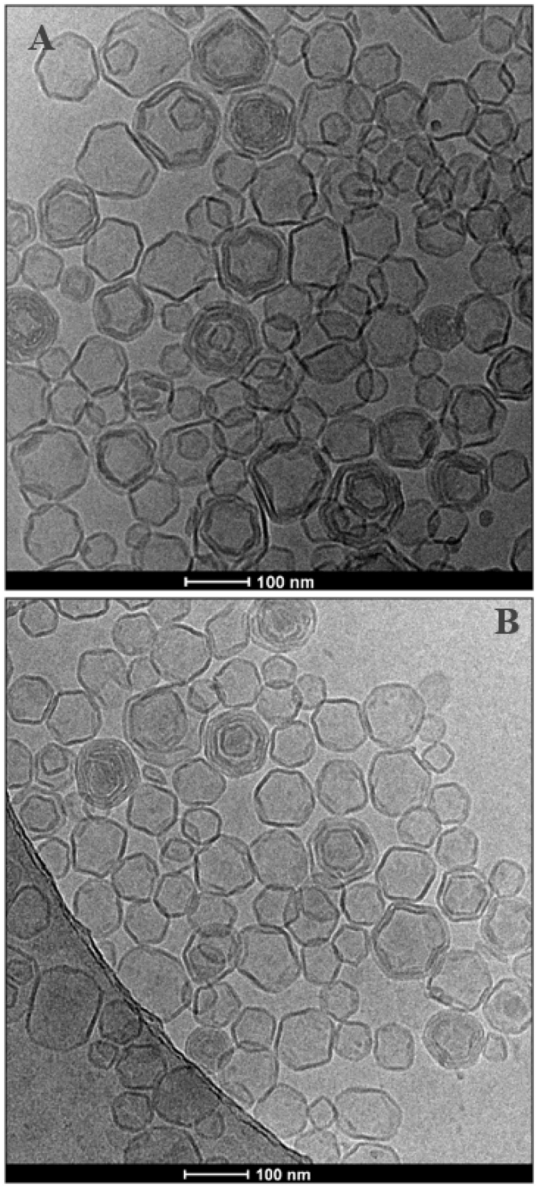

Fig. 6. Cryo-TEM images of DPPC vesicles prior (image A) and after (image B) the recalibration process of 140 nm liposomes through membrane with 50 nm pores performed at 20 °C.

phase transition but does not change further with falling temperature [19]. At the same time the cohesive forces increase continuously with decreasing temperature. To study the dependence of the lipid state on the liposome recalibration processes different experiments had been designed. During the experiment, the pre-calibrated liposomes (140 nm in size) were recalibrated through the filter with 50 nm pores. Measured extrusion forces, average sizes and PDI of resulting liposomes are presented in Fig. 5B and D. Presented data show that the extrusion force and the average liposome size depend on the extrusion temperature. The average size of recalibrated liposomes increases monotonically with decreasing temperature reaching, at about 20 °C, the initial value of 140 nm. Cryo-TEM images (Fig. 6) shows that DPPC vesicles were almost uniformly unilamellar, had similar sizes and topology characteristic for liposomes in the gel phase. Fig. 6A and B show images of 140 nm liposomes prior and after recalibration through 50 nm pores at 20 °C (gel phase), respectively. The comparison of the two images shows that neither topology nor size of liposomes were altered.

As already showed by Hope et al. [41] the extrusion of large lipid vesicles through 100-nm pores resulted in an average vesicle size of 140 nm. This outcome can be explained by assuming that, when entering the extrusion pore, lipid forms elongated tubular structure. The elongated tubular vesicle in extrusion pore [38,39] changes its shape into undulated necklace-like topology (Fig. 7). When leaving the extrusion pore, on the trans side, the necklace-like structures are transformed into separated spherical vesicles [42]. The ratio of the sphere and tube diameters during vesicles shape transformations shown in Fig. 7 had been calculated to be equal 1.37, 1.42 and 1.44 for reduced volumes equal $2^{-1/2}$, $3^{-1/2}$ and $4^{-1/2}$, respectively. The ratio increases for the lower reduced volume v, i.e. longer tubular vesicles. The predicted ratio of 1.4, from theoretically derived shapes (Fig. 7), may thus explain why vesicles extruded through 100 nm pore have the average diameter around 140 nm. Consequently, the mechanism of vesicle recalibration process can be described in terms of vesicle topological transformations, when entering and leaving the extrusion pore (Fig. 7). Specifically, elongated vesicles flow through the extrusion pore followed by the release of the undulated necklace-like structures on the extrusion pore trans side (Fig. 7), which finally transforms into separated spherical vesicles. Prior to this process, the lipid vesicles deform at some energy cost [39], when entering much smaller extrusion cylindrical pore. The lipid bilayer would not rupture when entering the extrusion pore only if the reduced volume of the large vesicle is smaller than 1.0. When inside the extrusion pore without the external force absent, the vesicle (membrane fragment) is undulated (necklace-like shape). At the presence of the extrusion force the vesicle (membrane fragment) is cylindrical (see also [43]). The elongated vesicle (membrane fragment) flow through the extrusion pore is governed by the viscous shear force and the value of the membrane free energy minimum [38,39]. The remaining part of the vesicle, which did not enter the extrusion pore, has elevated value of the relative volume (close to 1.0) and can participate in the next extrusion cycles only if its reduced volume decreases as a result of the tension induced transient membrane pore formation [44]. The elongated lipid vesicle inside the cylindrical extrusion pore aligns along the main symmetry axis of the pore and attains axisymmetric shape with the axis of symmetry parallel to the axis of the pore [37]. The reduced volume of the elongated vesicle, which is moving through the pore decreases slightly due to elastic stretching of its membrane in the field of the viscous shear force inside the extrusion pore [37]. When elongated tubular vesicles reach the end of the pore they adopt the undulated (necklace-like) shape with increased bending energy (Fig. 7), which is gained from the released membrane lateral stretching energy caused by the disappearance of the viscous shear force outside the pore. Finally, necklace-like structures outside the pore transform into separated spherical vesicles, process powered by the curvature induced frustration in the necks of the undulated necklace-like vesicle [42]. Note that the theoretically predicted shape transformations between the elongated tubular vesicles in the extrusion pore (left column in Fig. 7) and the necklace-like vesicles on the trans side of the pore (right column in Fig. 7) did not account for the effect of viscous forces on the shape of a vesicle flowing inside the extrusion pore [45].

The minimal pressure, generated on the cis side of the membrane as required for the sustainable volumetric flux, will depend predominantly on liposome reorganization at the pore entrance and visco-elastic properties of the medium inside the extrusion pore. If the viscosity of the liposome suspension in the pore can be neglected and the recalibration process does not change the size of the vesicle, the estimated bending rigidity of the membrane in gel phase equals to about 10^{-18} J, the value similar to that presented by others using macrovesicles as the model system ($1.35{\cdot}10^{-18}$ J [28]; $1.55{\cdot}10^{-18}$ J [21]). There are no reliable experimental evidences showing that the mechanical properties of a lipid bilayer can be translated from the microscale down to the submicron scale other than result presented in the paper. Experimental results presented in the paper can be interpreted in terms of the membrane bending rigidity and the cohesion of the lipid bilayer. The

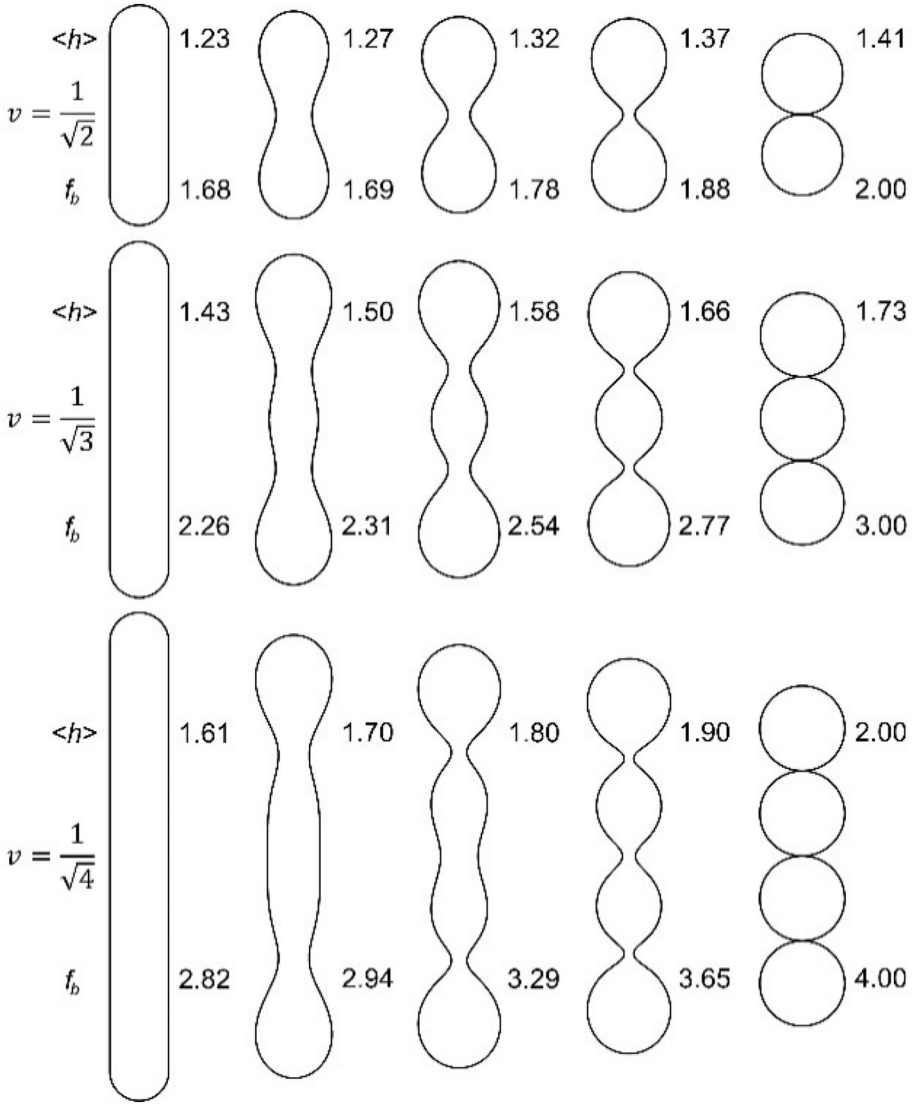

Fig. 7. The axisymmetric prolate vesicle shapes corresponding to the minimal local bending energy calculated for different values of reduced average mean curvatures $\langle h \rangle = 1/A \int (C_1 + C_2) dA$ and three values of the reduced volume v. The values of reduced local bending energy $f_b = F_b/8\pi k_c$ are also given for each shape, where F_b is the local bending energy of the vesicle and k_c is the bending constant (rigidity) of the bilayer membrane. Reduced volume is defined as $v = V/(4\pi R^3/3)$, where $R = \sqrt{A/4\pi}$ and A the vesicle surface area. The numerical calculation of the shapes corresponding to the minimal local bending energy was performed similarly as described in [48,57].

membrane cohesion affects its mechanics to such an extent that 140 nm vesicle in the gel phase passes unchanged through the 50 nm pore, whereas the same size vesicles in the fluid phase are recalibrated down to 80 nm. The entry of the vesicle into and flow through the extrusion pore can be related to the decrease of the reduced vesicle volume enforced by the tension induced transient membrane lipid pore formation (see also Karatekin et al. [44] and references therein). It is expected, that lipid pores in the membrane of tubular structure will reseal while it moves through the cylindrical extrusion pore. The dependences of the extrusion force and liposome size on temperature demonstrate that, when in the fluid phase membrane mechanics change little with temperature, in the gel phase the effect of temperature is different and depends on the system distance from the main phase transition. Previous experiments, using surface topology-sensitive fluorescent probe (fluorescein-PE), also demonstrated that the state of the lipid bilayer in the “gel phase” is a complex function of temperature [46].

4. Conclusion

Lipid bilayer mechanics attracts growing interest since its role in many cellular processes such as endocytosis, formation and stabilization of tubular membrane structures in the Golgi, change in the topology of nuclear envelope or membrane invagination in caveolae have been indicated [47–52]. The lipid bilayer mechanics is also an important property of liposome-based targeted drug delivery systems. The vesicle internalization by competent and/or targeted cells depends on their mechanics and shape [53]. The lipid bilayer state influences the corona formation affecting the liposome fate inside the body as well as triggering cargo release [54–56]. The lipid bilayer mechanics is an important factor in the designing of liposomes production processes, which require application of mechanical force as is the case in extrusion or homogenization techniques [34]. Mechanics of the lipid bilayer have been studies previously almost exclusively using micro-vesicles. It was not clear however, if parameters derived using such an experiment model can be translated to the nanoscale. The new experimental approach presented in the paper shows that there are no significant differences between the two experimental models when the bending rigidity coefficient of a lipid bilayer is evaluated. In addition, the presented experimental method, when combined with the conceptual model of vesicle formation, allows for the extraction a new quantitative

parameter (effective viscosity), which cannot be measured with other technique.

Transparency document

The Transparency document associated with this article can be found, in online version.

Declaration of competing interest

There are no conflicts to declare.

Acknowledgements

This study received financial support by Polish National Budget Funds for Science as a research project under the “Diamond Grant” program (Grant No. 0120/DIA/2018/47) to JD and a Grant POIR.04.01.04-00-0159/17-00 to MP, ML, PD, AF and BT by the National Centre for Research and Development (NCBiR). LM and AI the financial support from the Grants No. P2-0232 from the Slovenian Research Agency (ARRS). AI also acknowledge the funding from the European Union's Horizon 2020 research and innovation programme VES4US No. 801338.

AI and LM are grateful to W. Góźdź for computer program for calculation of equilibrium vesicles shapes.

References

[1] D. Van Swaay, A. Demello, Lab Chip 13 (2013) 752–767.
[2] C. Caddeo, L. Pucci, M. Gabriele, C. Carbone, X. Fernàndez-Busquets, D. Valenti, R. Pons, A. Vassallo, A.M. Fadda, M. Manconi, Int. J. Pharm. 538 (2018) 40–47.
[3] N. Shimokawa, M. Nagata, M. Takagi, Phys. Chem. Chem. Phys. 17 (2015) 20882–20888.
[4] J.C. Mathai, S. Tristram-Nagle, J.F. Nagle, M.L. Zeidel, J. Gen. Physiol. 131 (2008) 69–76.
[5] R. Dimova, Adv. Colloid Interf. Sci. 208 (2014) 225–234.
[6] K. Makino, A. Shibata, Adv. Planar Lipid Bilayers Liposomes 4 (2006) 49–77.
[7] M. Przybyło, T. Borowik, M. Langner, Liposomes Anal. Methodol. (2016) 345–383.
[8] H. Bouvrais, Adv. Planar Lipid Bilayers Liposomes 15 (2012) 1–75.
[9] W. Rawicz, K.C. Olbrich, T. McIntosh, D. Needham, E.A. Evans, Biophys. J. 79 (2000) 328–339.
[10] S. Garcia-manyes, L. Redondo-morata, G. Oncins, J. Am. Chem. Soc. 132 (2010) 12874–12886.
[11] P.S. Niemelä, M.T. Hyvönen, I. Vattulainen, Biophys. J. 90 (2006) 851–863.
[12] N. Kučerka, S. Tristram-Nagle, J.F. Nagle, J. Membr. Biol. 208 (2006) 193–202.
[13] H. He, Y. Lu, J. Qi, Q. Zhu, Z. Chen, W. Wu, Acta Pharm. Sin. B 9 (2019) 36–48.
[14] D. Lombardo, P. Calandra, D. Barreca, S. Magazù, M. Kiselev, Nanomaterials 6 (2016) 125.
[15] S. Zhang, H. Gao, G. Bao, ACS Nano 9 (2015) 8655–8671.
[16] X. Yi, X. Shi, H. Gao, Phys. Rev. Lett. 107 (2011).
[17] K.J. Van Vliet, G. Bao, S. Suresh, Acta Mater. 51 (2003) 5881–5905.
[18] L. Scheffer, A. Bitler, E. Ben-Jacob, R. Korenstein, Eur. Biophys. J. 30 (2001) 83–90.
[19] A.F. Loftus, S. Noreng, V.L. Hsieh, R. Parthasarathy, Langmuir 29 (2013) 14588–14594.
[20] L.A. Bagatolli, D. Needham, Chem. Phys. Lipids 181 (2014) 99–120.
[21] O. Et-Thakafy, N. Delorme, C. Gaillard, C. Mériadec, F. Artzner, C. Lopez, F. Guyomarch, Langmuir 33 (2017) 5117–5126.
[22] C.M. Franz, P.-H. Puech, Cell. Mol. Bioeng. 1 (2008) 289–300.
[23] B.R. Brückner, A. Janshoff, Biochim. Biophys. Acta - Mol. Cell Res. 1853 (2015) 3075–3082.
[24] K.A. Riske, R.P. Barroso, C.C. Vequi-Suplicy, R. Germano, V.B. Henriques, M.T. Lamy, Biochim. Biophys. Acta Biomembr. 1788 (2009) 954–963.
[25] C.H. Lee, W.C. Lin, J. Wang, Phys. Rev. E - Stat. Physics, Plasmas, Fluids, Relat. Interdiscip. Top. 64 (2001) 4.
[26] N. Michel, A.S. Fabiano, A. Polidori, R. Jack, B. Pucci, Chem. Phys. Lipids 139 (2006) 11–19.
[27] T. Kaasgaard, C. Leidy, J.H. Crowe, O.G. Mouritsen, K. Jørgensen, Biophys. J. 85 (2003) 350–360.
[28] R.M. Venable, F.L.H. Brown, R.W. Pastor, Chem. Phys. Lipids 192 (2015) 60–74.
[29] J. Pan, S. Tristram-Nagle, N. Kučerka, J.F. Nagle, Biophys. J. 94 (2008) 117–124.
[30] A.D. Bangham, J. De Gier, G.D. Greville, Chem. Phys. Lipids 1 (1967) 225–246.
[31] F. Olson, C.A. Hunt, F.C. Szoka, W.J. Vail, D. Papahadjopoulos, BBA - Biomembr 557 (1979) 9–23.
[32] S.G.M. Ong, M. Chitneni, K.S. Lee, L.C. Ming, K.H. Yuen, Pharmaceutics 8 (2016).
[33] J.C.M. Stewart, Anal. Biochem. 104 (1980) 10–14.
[34] P. Guo, J. Huang, Y. Zhao, C.R. Martin, R.N. Zare, M.A. Moses, Small 14 (2018).
[35] R. Nayar, M.J. Hope, P.R. Cullis, BBA - Biomembr 986 (1989) 200–206.
[36] A. Hinna, F. Steiniger, S. Hupfeld, P. Stein, J. Kuntsche, M. Brandl, J. Liposome Res. 26 (2016) 11–20.
[37] V. Vitkova, M. Mader, T. Podgorski, Europhys. Lett. 68 (2004) 398–404.
[38] R. Bruinsma, Phys. A Stat. Mech. Its Appl. 234 (1996) 249–270.
[39] D.G. Hunter, B.J. Frisken, Biophys. J. 74 (1998) 2996–3002.
[40] M. Ibarguren, A. Alonso, B.G. Tenchov, F.M. Goñi, Biochim. Biophys. Acta Biomembr. 1798 (2010) 1735–1738.
[41] M.J. Hope, M.B. Bally, G. Webb, P.R. Cullis, BBA - Biomembr 812 (1985) 55–65.
[42] D. Jesenek, Š. Perutková, W. Góźdź, V. Kralj-Iglič, A. Iglič, S. Kralj, Int. J. Nanomedicine 8 (2013) 677–687.
[43] L. Mesarec, W. Góźdź, S. Kralj, M. Fošnarič, S. Penič, V. Kralj-Iglič, A. Iglič, Eur. Biophys. J. 46 (2017) 705–718.
[44] E. Karatekin, O. Sandre, H. Guitouni, N. Borghi, P.H. Puech, F. Brochard-Wyart, Biophys. J. 84 (2003) 1734–1749.
[45] D. Abreu, M. Levant, V. Steinberg, U. Seifert, Adv. Colloid Interf. Sci. 208 (2014) 129–141.
[46] M. Langner, H. Pruchnik, K. Kubica, Zeitschrift Fur Naturforsch. - Sect. C J. Biosci. 55 (2000) 418–424.
[47] H. Alimohamadi, P. Rangamani, Biomolecules 8 (2018).
[48] J.E. Hassinger, G. Oster, D.G. Drubin, P. Rangamani, Proc. Natl. Acad. Sci. U. S. A. 114 (2017) E1118–E1127.
[49] N. Bobrovska, W. Góźdź, V. Kralj-Iglič, A. Iglič, PLoS One 8 (2013).
[50] M. Torbati, T.P. Lele, A. Agrawal, Proc. Natl. Acad. Sci. U. S. A. 113 (2016) 11094–11099.
[51] X. Liang, Y. Zu, Y.P. Cao, C. Yang, Soft Matter 9 (2013) 7981–7987.
[52] J.C. Stachowiak, F.M. Brodsky, E.A. Miller, Nat. Cell Biol. 15 (2013) 1019–1027.
[53] B. Yameen, W. Il Choi, C. Vilos, A. Swami, J. Shi, O.C. Farokhzad, J. Control. Release 190 (2014) 485–499.
[54] C. Corbo, R. Molinaro, M. Tabatabaei, O.C. Farokhzad, M. Mahmoudi, Biomater. Sci. 5 (2017) 378–387.
[55] N. Bertrand, P. Grenier, M. Mahmoudi, E.M. Lima, E.A. Appel, F. Dormont, J.M. Lim, R. Karnik, R. Langer, O.C. Farokhzad, Nat. Commun. 8 (2017).
[56] U. Kauscher, M.N. Holme, M. Björnmalm, M.M. Stevens, Adv. Drug Deliv. Rev. 138 (2019) 259–275.
[57] W.T. Góźdź, Langmuir 20 (2004) 7385–7391.